BULLETIN OF THE POLISH ACADEMY OF SCIENCES
TECHNICAL SCIENCES, Vol. 61, No. 2, 2013
DOI: 10.2478/bpasts-2013-0047

Effect of the mathematical model and integration step on the accuracy of the results of computation of artillery projectile flight parameters

L. BARANOWSKI*

Faculty of Mechatronics and Aerospace, Military University of Technology, 2 Kaliskiego St., 00-908 Warsaw, Poland

Abstract. In the paper the three different mathematical models of motion of a spin-stabilized, conventional artillery projectile, possessing at least trigonal symmetry, have been introduced. The vector six-degrees-of-freedom (6-DOF) differential equations of motion are an updated edition of those published by Lieske and McCoy and are consistent with STANAG 4355 (Ed. 3). The mathematical models have been used to developing software for simulating the flight of the Denel 155mm Assegai M2000 series artillery projectile and to conduct comprehensive research of the influence of the applied model and integration step on the accuracy and time of computation of projectile trajectory.

Key words: exterior ballistics, fight dynamics, equations of motion of the projectile, mathematical model.

1. Introduction

The model representing the projectile as a rigid body with six degrees of freedom is the main mathematical model (in short 6-DOF model) that enables testing dynamic properties of motion of ground artillery projectiles [1]. Typically, modeling assumes that the projectile is exposed to full aerodynamic force, including the Magnus force and moment, gravity force, Coriolis force caused by the Earth's rotation and, possibly, rocket engine thrust (for projectiles with propulsion). Much of the form of the mathematical model depends on: the coordinate system used to derive of dynamic projectile motion equations, angles that are used for describing aerodynamic forces and moments and the method of constructing kinematic equations of motion.

Literature, mainly that concerned with aviation technologies, uses mostly Euler angles or quasi-Euler angles (often called as aviation angles in the context of flight dynamics [2, 3]) but also, increasingly more frequently, Euler [4, 5], Rodriguez-Hamilton [6] or Cayley-Klein [4–6] parameters for constructing kinematic equations of motion (or kinematic relations). Selecting a mathematical form of kinematic equations of motion is motivated by the wish to avoid numerical singularities (division by zero) for some object positions in space. Using kinematic direction cosines for projectile axes of symmetry [7] can be an alternative to using Euler angles and parameters.

Principles of classical mechanics are used in developing the 6DOF model. They are often used when constructing the equations of motion of flying objects [2, 8] which are the alternative to methods based on the principles of analytical mechanics. Among these methods we can distinguish ones based on inertial generalized coordinates and referring directly to Hamilton's principle or Lagrange equations [9], and methods involving the use of equations of analytical mechanics in quasi-coordinates e.g. Boltzmann-Hamel equations [10].

The paper presents the following 6-DOF mathematical models different in both dynamic and kinematic equations of motion and the methods of describing aerodynamic forces and moments acting on the projectile in flight:

1. Model using the ground-fixed system: equations for both translational and rotational motion are derived in the ground-fixed system O_0123 (Fig. 1), kinematic equations of rotational motion are used direction cosines of the axes of symmetry of the projectile instead of quasi-Euler angles, while aerodynamic forces and moments are determined basing on the total angle of attack α_t (Fig. 1) [7, 11];
2. Model using the body axis system: equations for both translational and rotational motion are derived in the body axis system *Oxyz*, kinematic equations of rotational motion are used quasi-Euler angles Ψ, Θ, Φ (often called as aviation angles), while aerodynamic forces and moments are determined using angle of attack α and angle of sideslip β [3];
3. Model using the velocity axis system: equations of motion of center of mass are derived in the velocity axis system $Ox_k y_k z_k$, equations of rotational motion about the center of mass are derived in the body axis system *Oxyz*, kinematic equations of rotational motion are used quasi-Euler angles Ψ, Θ, Φ, while aerodynamic forces and moments are determined using angle of attack α and angle of sideslip β.

The foregoing mathematical models have been used to developing software for simulating the flight of the Denel 155 mm artillery projectile (Assegai M2000 series) and to conduct comprehensive research of the influence of the applied model and integration step on the accuracy and time of computation of projectile trajectory.

*e-mail: leszek.baranowski@wat.edu.pl

2. Mathematical model of flight dynamics of the projectile as a rigid body in the ground-fixed system

The mathematical model of flight dynamics of the projectile as a rigid body in the ground-fixed system uses the right-handed orthonormal Cartesian coordinate system O_0123 referenced to the gun position (Fig. 1), defined in STANAG 4355 ed. 3. The location of the projectile center of mass relative to the ground-fixed system is defined by vector $\mathbf{X}$. The vector of velocity of the projectile relative to air $\mathbf{v}$ is the difference between the vector of velocity of the projectile relative to the ground $\mathbf{u}$ and the vector of velocity of wind $\mathbf{w}$.

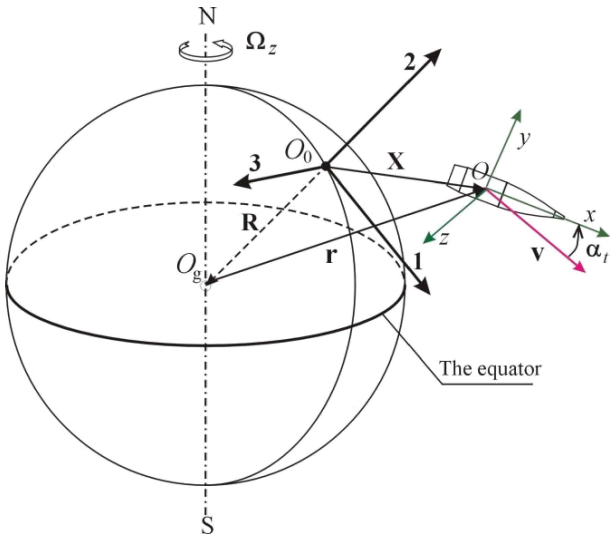

Fig. 1. Projectile position relative to the ground-fixed system O_0123

The description of aerodynamic forces and moments affecting the projectile in flight use the total angle of attack α_t contained between the longitudinal axis of the projectile Ox and the vector of velocity of the projectile relative to air $\mathbf{v}$ (Fig. 1) and two unit vectors (versors) $\mathbf{x}$ and $\mathbf{i}_V$ applied to the center of mass of the projectile:

- Unit vector $\mathbf{x}$ runs along the axis of symmetry of the projectile towards the tip (Fig. 1), in the ground-fixed system it has components identified as follows $\mathbf{x} = [x_1, x_2, x_3]$;
- Unit vector $\mathbf{i}_V$ runs along the axis overlapping with the vector of velocity of the projectile relative to air $\mathbf{v}$, in the ground-fixed system it has components identified as follows $\mathbf{v} = [v_1, v_2, v_3]$ and $v = \sqrt{v_1^2 + v_2^2 + v_3^2}$.

2.1. Vector form of equations of projectile motion in the ground-fixed system. In the ground-fixed system, vector differential equations of motion of the projectile as a rigid body can be derived from the law of change of linear momentum $m\mathbf{u}$ and of angular momentum of the body relative to the projectile center of mass $\mathbf{H}$. The total angular momentum of the rotationally symmetric body can now be expressed as the sum of two vectors [7]:

- the angular momentum about $\mathbf{x}$ (spin axis):

$$I_x p\mathbf{x}, \tag{1a}$$

- and the angular momentum about an axis perpendicular to $\mathbf{x}$:

$$I_y(\mathbf{x} \times \frac{d\mathbf{x}}{dt}), \tag{1b}$$

where p is the rate of roll (axial spin), I_x is the moment of inertia about the spin axis, and I_y is the moment of inertia about any axis perpendicular to the spin axis.

Therefore, the total angular momentum of the projectile can be represented by the vector:

$$\mathbf{H} = I_x p\mathbf{x} + I_y(\mathbf{x} \times \frac{d\mathbf{x}}{dt}). \tag{2}$$

In its final vector form, the mathematical model contains the following groups of equations [11]:

- Vector differential equations of motion of the projectile center of mass:

$$m\frac{d\mathbf{u}}{dt} = \mathbf{DF} + \mathbf{LF} + \mathbf{MF} + m\mathbf{g} + m\mathbf{\Lambda}, \tag{3a}$$

$$\frac{d\mathbf{X}}{dt} = \mathbf{u}. \tag{3b}$$

- Vector differential equations of rotational motion about the projectile center of mass:

$$\frac{d\mathbf{H}}{dt} = \mathbf{OM} + \mathbf{PDM} + \mathbf{MM} + \mathbf{SDM}, \tag{4a}$$

$$\frac{d\mathbf{x}}{dt} = \frac{(\mathbf{H} \times \mathbf{x})}{I_y}. \tag{4b}$$

Aerodynamic forces and moments occurring in the equations of motion were defined according to the BRL Aeroballistic System [7] while retaining conformity of the notation with STANAG 4355 [11], a NATO official standardization agreement.

The aerodynamic drag force **DF** opposes the forward velocity of the projectile is given as Eq. (5a), and the scalar magnitude of the force is stated as Eq. (5b):

$$\mathbf{DF} = -(C_{D_0} + C_{D_{\alpha^2}} \sin^2 \alpha_t)\frac{\rho v^2}{2} S\mathbf{i}_V, \tag{5a}$$

$$DF = -(C_{D_0} + C_{D_{\alpha^2}} \sin^2 \alpha_t)\frac{\rho v^2}{2} S, \tag{5b}$$

where C_{D_0} – zero-yaw drag coefficient, $C_{D_{\alpha^2}}$ – yaw drag coefficient, ρ – air density, S – the reference area.

The aerodynamic lift force **LF** is proportional to the sine of the total angle of attack and always acts perpendicular to the trajectory in the plane containing both the trajectory and the projectile axis of rotational symmetry. The lift force is stated in vector and scalar forms:

$$\mathbf{LF} = (C_{L_\alpha} + C_{L_{\alpha^3}} \sin^2 \alpha_t)\frac{\rho v^2}{2} S\left[\mathbf{i}_V \times (\mathbf{x} \times \mathbf{i}_V)\right], \tag{6a}$$

$$LF = (C_{L_\alpha} + C_{L_{\alpha^3}} \sin^2 \alpha_t)\frac{\rho v^2}{2} S \sin \alpha_t, \tag{6b}$$

where C_{L_α} – linear lift force coefficient, $C_{L_{\alpha^3}}$ – cubic lift force coefficient.

The Magnus force **MF** is produced by unequal pressures on opposite sides of a spinning body. The unequal pressures are the result of viscous interaction between the fluid and

spinning surface. The Magnus force always acts in a direction perpendicular to the plane of total angle of attack. The vector and scalar equations defining the Magnus force are:

$$\mathbf{MF} = \frac{\rho v^2}{2} S \left(\frac{pd}{v}\right) C_{mag-f} (\mathbf{i}_V \times \mathbf{x}), \tag{7a}$$

$$MF = C_{mag-f} \frac{\rho v^2}{2} S \left(\frac{pd}{v}\right) \sin\alpha_t \tag{7b}$$

where C_{mag-f} – Magnus force coefficient, $\frac{pd}{v}$ – normalized rate of roll, d – the projectile reference diameter.

The Magnus moment $\mathbf{MM}$ can be either positive or negative, depending on the projectile shape, the center of mass location, the amplitude of α_t and the flight Mach number. The Magnus moment is defined by the vector and scalar equations:

$$\mathbf{MM} = \frac{\rho v^2}{2} Sd \left(\frac{pd}{v}\right) C_{mag-m} \left[\mathbf{x} \times (\mathbf{i}_V \times \mathbf{x})\right], \tag{8a}$$

$$MM = \frac{\rho v^2}{2} Sd \left(\frac{pd}{v}\right) C_{mag-m} \sin\alpha_t, \tag{8b}$$

where C_{mag-m} – Magnus moment coefficient.

The overturning moment **OM** is the aerodynamic moment associated with the lift force. If the projectile nose lies above its trajectory, a positive overturning moment acts to increase the total angle of attack. The overturning moment is given by the vector and scalar equations:

$$\mathbf{OM} = \left(C_{M_\alpha} + C_{M_{\alpha^3}} \sin^2\alpha_t\right) \frac{\rho v^2}{2} Sd (\mathbf{i}_V \times \mathbf{x}), \tag{9a}$$

$$OM = \left(C_{M_\alpha} + C_{M_{\alpha^3}} \sin^2\alpha_t\right) \frac{\rho v^2}{2} Sd \sin\alpha_t, \tag{9b}$$

where C_{M_α} – overturning moment coefficient, $C_{M_{\alpha^3}}$ – cubic overturning moment coefficient.

The spin damping moment $\mathbf{SDM}$ opposes the spin of the projectile; it always reduces the axial spin. The vector spin damping moment is defined as Eq. (10a), and the scalar magnitude is given by Eq. (10b)

$$\mathbf{SDM} = \frac{\rho v^2}{2} Sd \left(\frac{pd}{v}\right) C_{spin} \mathbf{x}, \tag{10a}$$

$$SDM = C_{spin} \frac{\rho v^2}{2} Sd \left(\frac{pd}{v}\right), \tag{10b}$$

where C_{spin} – spin damping moment coefficient.

The pitch damping moment **PDM** contains two parts, one part proportional to transverse angular velocity q_t and a second part proportional to the rate of change of the total angle of attack $\dot{\alpha}_t$. Because of q_t and $\dot{\alpha}_t$ are virtually identical in practice, and the pitch damping moment is well approximated by expressions:

$$\mathbf{PDM} = \frac{1}{2} Sd^2 v \left(C_{M_q} + C_{M_{\dot\alpha}}\right) \left(\mathbf{x} \times \frac{d\mathbf{x}}{dt}\right), \tag{11a}$$

$$PDM = \frac{\rho v^2}{2} Sd \left(\frac{q_t d}{v}\right) \left(C_{M_q} + C_{M_{\dot\alpha}}\right), \tag{11b}$$

where C_{M_q} – pitch damping moment coefficient due to q_t, $C_{M_{\dot\alpha}}$ – pitch damping moment coefficient due to $\dot{\alpha}_t$.

Using the vector calculus rules and substitution $\mathbf{v} = v\mathbf{i}_V$, $S = \pi d^2/4$, $p = (\mathbf{H} \cdot \mathbf{x}) / I_x$, $(\mathbf{x} \times \frac{d\mathbf{x}}{dt}) = (\mathbf{H} - I_x p \mathbf{x}) / I_y$ equations (5)–(11) can be transformed to the following form:

$$\mathbf{DF} = -\frac{\pi\rho d^2}{8} (C_{D_0} + C_{D_{\alpha^2}} \sin^2\alpha_t) v\mathbf{v}, \tag{12}$$

$$\mathbf{LF} = \frac{\pi\rho d^2}{8} (C_{L_\alpha} + C_{L_{\alpha^3}} \sin^2\alpha_t) \left[v^2\mathbf{x} - (\mathbf{v} \cdot \mathbf{x})\mathbf{v}\right], \tag{13}$$

$$\mathbf{MF} = \frac{\pi\rho d^3}{8I_x} C_{mag-f} (\mathbf{H} \cdot \mathbf{x}) (\mathbf{v} \times \mathbf{x}), \tag{14}$$

$$\mathbf{MM} = \frac{\pi\rho d^4}{8I_x} C_{mag-m} (\mathbf{H} \cdot \mathbf{x}) \left[\mathbf{v} - (\mathbf{v} \cdot \mathbf{x})\mathbf{x}\right], \tag{15}$$

$$\mathbf{OM} = \frac{\pi\rho v d^3}{2} \left(C_{M_\alpha} + C_{M_{\alpha^3}} \sin^2\alpha_t\right) (\mathbf{v} \times \mathbf{x}), \tag{16}$$

$$\mathbf{SDM} = \frac{\pi\rho d^4 v}{8I_x} C_{spin} (\mathbf{H} \cdot \mathbf{x}) \mathbf{x}, \tag{17}$$

$$\mathbf{PDM} = \frac{\pi\rho d^4 v}{8I_y} \left(C_{M_q} + C_{M_{\dot\alpha}}\right) \left[\mathbf{H} - (\mathbf{H} \cdot \mathbf{x})\mathbf{x}\right]. \tag{18}$$

A spherical model of the Earth is given, the gravity force vector can be presented in the ground-fixed system as follows:

$$\begin{aligned} m\mathbf{g} = -mg_0 \left(R^2/r^3\right) \mathbf{r} = m \begin{bmatrix} g_1 \\ g_2 \\ g_3 \end{bmatrix} \\ = -mg_0 \begin{bmatrix} X_1/R \\ 1 - 2X_2/R \\ X_3/R \end{bmatrix}, \end{aligned} \tag{19}$$

where $\mathbf{r} = \mathbf{X} - \mathbf{R}$ – defines the position of the projectile relative to the center of mass of the Earth, $R = 6356766$ [m] – radius of the sphere, locally approximating the geoid, $g_0 = 9.80665(1 - 0.0026\cos(2lat))$ [m/s^2] – magnitude of acceleration due to gravity at mean sea level, *lat* – latitude of launch point; for southern hemisphere *lat* is negative [deg].

The Coriolis force can be expressed with the following known equation:

$$m\mathbf{\Lambda} = -2m (\mathbf{\Omega}_z \times \mathbf{u}), \tag{20}$$

where $\mathbf{\Omega}_z$ –vector of angular velocity of the earth and its components in ground-fixed system O_0123,

$$\mathbf{\Omega}_z = \begin{bmatrix} \Omega_{z1} \\ \Omega_{z2} \\ \Omega_{z3} \end{bmatrix} = \begin{bmatrix} \Omega_z \cos(lat)\cos(AZ) \\ \Omega_z \sin(lat) \\ -\Omega_z \cos(lat)\sin(AZ) \end{bmatrix}, \tag{21}$$

$\Omega_z = 7.292115\ 10^{-5}$ [rad/s] – angular speed of the earth, AZ – Azimuth (Bearing) of O_01 axis measured clockwise from true North [mil].

2.2. Scalar form of equations of projectile motion in the ground-fixed system. The scalar form of equations of projectile motion have been obtained by projecting vector equations (both translational and rotational motion) on the axes of the ground-fixed coordinate system O_0123. So construed mathematical model is a system of differential-algebraic equations including:

– Dynamic differential equations of motion of the projectile center of mass derived from Eq. (3a):

$$\begin{aligned}\frac{du_1}{dt} &= -\left(\frac{\pi\rho d^2}{8m}\right)\left(C_{D_0}+C_{D_{\alpha^2}}\sin^2\alpha_t\right)vv_1\\ &+\left(\frac{\pi\rho d^2}{8m}\right)\left(C_{L_\alpha}+C_{L_{\alpha^3}}\sin^2\alpha_t\right)\left(v^2x_1-vv_1\cos\alpha_t\right)\\ &-\frac{\pi\rho d^3C_{mag-f}}{8mI_x}\left(H_1x_1+H_2x_2+H_3x_3\right)\left(x_2v_3-x_3v_2\right)\\ &-g_0\frac{X_1}{R}-2\Omega\left(\sin(lat)u_3+\cos(lat)\sin(AZ)u_2\right),\end{aligned} \tag{22a}$$

$$\begin{aligned}\frac{du_2}{dt} &= -\left(\frac{\pi\rho d^2}{8m}\right)\left(C_{D_0}+C_{D_{\alpha^2}}\sin^2\alpha_t\right)vv_2\\ &+\left(\frac{\pi\rho d^2}{8m}\right)\left(C_{L_\alpha}+C_{L_{\alpha^3}}\sin^2\alpha_t\right)\left(v^2x_2-vv_2\cos\alpha_t\right)\\ &-\frac{\pi\rho d^3C_{mag-f}}{8mI_x}\left(H_1x_1+H_2x_2+H_3x_3\right)\left(x_3v_1-x_1v_3\right)\\ &-g_0\left(1-\frac{2X_2}{R}\right)\\ &+2\Omega\left(\cos(lat)\sin(AZ)u_1+\cos(lat)\cos(AZ)u_3\right),\end{aligned} \tag{22b}$$

$$\begin{aligned}\frac{du_3}{dt} &= -\left(\frac{\pi\rho d^2}{8m}\right)\left(C_{D_0}+C_{D_{\alpha^2}}\sin^2\alpha_t\right)vv_3\\ &+\left(\frac{\pi\rho d^2}{8m}\right)\left(C_{L_\alpha}+C_{L_{\alpha^3}}\sin^2\alpha_t\right)\left(v^2x_3-vv_3\cos\alpha_t\right)\\ &-\frac{\pi\rho d^3C_{mag-f}}{8mI_x}\left(H_1x_1+H_2x_2+H_3x_3\right)\left(x_1v_2-x_2v_1\right)\\ &-g_0\left(\frac{X_3}{R}\right)-2\Omega\left(\cos(lat)\cos(AZ)u_2-\sin(AZ)u_1\right).\end{aligned} \tag{22c}$$

– Kinematic differential equations of motion of the projectile center of mass derived from Eq. (3b):

$$\frac{dX_1}{dt} = u_1, \tag{23a}$$

$$\frac{dX_2}{dt} = u_2, \tag{23b}$$

$$\frac{dX_3}{dt} = u_3. \tag{23c}$$

– Dynamic differential equations of rotational motion about the projectile center of mass derived from Eq. (4a):

$$\begin{aligned}\frac{dH_1}{dt} &= \frac{\pi\rho vd^3}{2}\left(C_{M_\alpha}+C_{M_{\alpha^3}}\sin^2\alpha_t\right)\left(v_2x_3-v_3x_2\right)\\ &+\frac{\pi\rho d^4v}{8I_y}\left(C_{M_q}+C_{M_{\dot\alpha}}\right)\left[H_1-\left(H_1x_1+H_2x_2+H_3x_3\right)x_1\right]\\ &+\frac{\pi\rho d^4}{8I_x}C_{mag-m}\left(H_1x_1+H_2x_2+H_3x_3\right)\left(v_1-vx_1\cos\alpha_t\right)\\ &+\frac{\pi\rho d^4v}{8I_x}C_{spin}\left(H_1x_1+H_2x_2+H_3x_3\right)x_1,\end{aligned} \tag{24a}$$

$$\begin{aligned}\frac{dH_2}{dt} &= \frac{\pi\rho vd^3}{2}\left(C_{M_\alpha}+C_{M_{\alpha^3}}\sin^2\alpha_t\right)\left(v_3x_1-v_1x_3\right)\\ &+\frac{\pi\rho d^4v}{8I_y}\left(C_{M_q}+C_{M_{\dot\alpha}}\right)\left[H_2-\left(H_1x_1+H_2x_2+H_3x_3\right)x_2\right]\\ &+\frac{\pi\rho d^4}{8I_x}C_{mag-m}\left(H_1x_1+H_2x_2+H_3x_3\right)\left(v_2-vx_2\cos\alpha_t\right)\\ &+\frac{\pi\rho d^4v}{8I_x}C_{spin}\left(H_1x_1+H_2x_2+H_3x_3\right)x_2,\end{aligned} \tag{24b}$$

$$\begin{aligned}\frac{dH_3}{dt} &= \frac{\pi\rho vd^3}{2}\left(C_{M_\alpha}+C_{M_{\alpha^3}}\sin^2\alpha_t\right)\left(v_1x_2-v_2x_1\right)\\ &+\frac{\pi\rho d^4v}{8I_y}\left(C_{M_q}+C_{M_{\dot\alpha}}\right)\left[H_3-\left(H_1x_1+H_2x_2+H_3x_3\right)x_3\right]\\ &+\frac{\pi\rho d^4}{8I_x}C_{mag-m}\left(H_1x_1+H_2x_2+H_3x_3\right)\left(v_3-vx_3\cos\alpha_t\right)\\ &+\frac{\pi\rho d^4v}{8I_x}C_{spin}\left(H_1x_1+H_2x_2+H_3x_3\right)x_3.\end{aligned} \tag{24c}$$

– Kinematic differential equations of rotational motion about the projectile center of mass for direction cosines derived from Eq. (4b):

$$\frac{dx_1}{dt} = \frac{\left(H_2x_3-H_3x_2\right)}{I_y}, \tag{25a}$$

$$\frac{dx_2}{dt} = \frac{\left(H_3x_1-H_1x_3\right)}{I_y}, \tag{25b}$$

$$\frac{dx_3}{dt} = \frac{\left(H_1x_2-H_2x_1\right)}{I_y}. \tag{25c}$$

– Equations defining the total angle of attack derived from the equation for scalar product:

$$\cos\alpha_t = \frac{\left(\mathbf{v}\cdot\mathbf{x}\right)}{v} = \frac{v_1x_1+v_2x_2+v_3x_3}{v}. \tag{26}$$

– Equations for components and absolute value of the vector of projectile velocity in air:

$$\begin{gathered}v_1 = u_1-w_1, \qquad v_2 = u_2-w_2, \qquad v_3 = u_3-w_3\\ v = \sqrt{v_1^2+v_2^2+v_3^2}.\end{gathered} \tag{27}$$

– Equations for initial conditions:

$$u_1(t=0) = MV\cos(QE)\cos(\Delta AZ),$$

$$u_2(t=0) = MV\sin(QE),$$

$$u_3(t=0) = MV\cos(QE)\sin(\Delta AZ),$$

$$x_1(t=0) = \cos(QE)\cos(\Delta AZ),$$

$$x_2(t=0) = \sin(QE),$$

$$x_3(t=0) = \cos(QE)\sin(\Delta AZ),$$

$$H_1(t=0) = I_x p_0 x_1 - I_y(q_0\sin(\Delta AZ) - r_0\sin(QE)\cos(\Delta AZ)),$$

$$H_2(t=0) = I_x p_0 x_2 - I_y r_0\cos(QE),$$

$$H_3(t=0) = I_x p_0 x_3 + I_y(q_0\cos(\Delta AZ) + r_0\sin(QE)\sin(\Delta AZ)),$$

where QE – vertical angle of the weapon barrel (quadrant elevation) [mil], ΔAZ – difference between the weapon azimuth (bearing) and the **1** axis measured clockwise [mil], MV – initial (muzzle) velocity [m/s], $p_0 = \frac{2\pi MV}{\eta d}$ – initial roll velocity about the x axis (initial rate of roll) [rad/s], q_0 – initial pitch velocity about the y axis (initial rate of pitch) [rad/s], r_0 – initial yaw velocity about the z axis (initial rate of yaw) [rad/s], η – the twist rate in the end of the gun barrel (expressed in calibers per revolution).

3. Mathematical models of flight dynamics of the projectile as a rigid body in systems moving together with the projectile

The modeling of flight dynamics of the projectile as a rigid body in systems moving together with the projectile uses the standard coordinate systems conforming to Polish and International Standard ISO 1151 [3] and the velocity axis system $Ox_k y_k z_k$ (Fig. 2) defined as follows: the origin of the system overlaps with the center of mass of the projectile, axis x_k follows the vector of velocity of the projectile relative to the ground **u**, axis z_k lays on the vertical plane crossing the vector of velocity **u** and is oriented down, axis y_k lays on the horizontal plane and completes the system to make it the right-handed one.

The determination of aerodynamic forces and moments affecting the projectile in flight uses the following: angle of attack α and angle of sideslip β. Then, the transformation matrix between the air-path axis system $Ox_a y_a z_a$ and the body axis system $Oxyz$ has the following form:

$$\mathbf{L}_{\alpha\beta} = \begin{bmatrix} \cos\alpha\cos\beta & \cos\alpha\sin\beta & -\sin\alpha \\ -\sin\beta & \cos\beta & 0 \\ \sin\alpha\cos\beta & \sin\alpha\sin\beta & \cos\alpha \end{bmatrix}. \tag{28}$$

The description of the vector of the projectile velocity **u** position relative to the normal earth axis system uses the following: azimuth angle of the projectile velocity χ, and inclination angle of the projectile velocity γ. The derived transformation matrix between the normal earth axis system $Ox_g y_g z_g$ and the velocity axis system $Ox_k y_k z_k$ has the following form:

$$\mathbf{L}_{\gamma\chi} = \begin{bmatrix} \cos\gamma\cos\chi & \cos\gamma\sin\chi & -\sin\gamma \\ -\sin\chi & \cos\chi & 0 \\ \sin\gamma\cos\chi & \sin\gamma\sin\chi & \cos\gamma \end{bmatrix}. \tag{29}$$

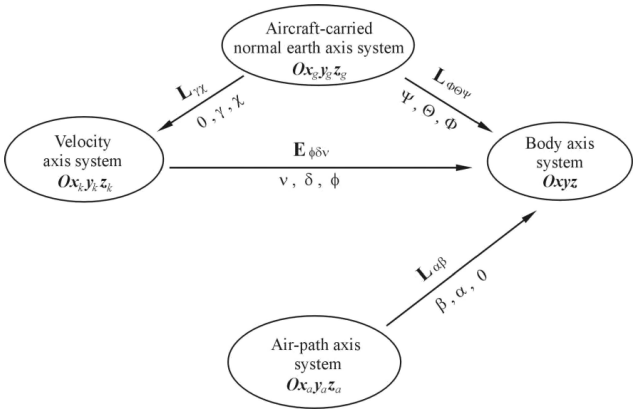

Fig. 2. Diagram of coordinate systems used for modeling and angular relations between the systems

The description of the projectile position relative to the normal earth axis system uses the following: azimuth angle Ψ, inclination angle Θ and bank angle Φ. The derived transformation matrix between the normal earth axis system $Ox_g y_g z_g$ and the body axis system $Oxyz$ has the following form:

$$\mathbf{L}_{\Phi\Theta\Psi} = \begin{bmatrix} \cos\Theta\cos\Psi & \cos\Theta\sin\Psi & -\sin\Theta \\ -\cos\Phi\sin\Psi + \sin\Phi\sin\Theta\cos\Psi & \cos\Phi\cos\Psi + \sin\Phi\sin\Theta\sin\Psi & \sin\Phi\cos\Theta \\ \sin\Phi\sin\Psi + \cos\Phi\sin\Theta\cos\Psi & -\sin\Phi\cos\Psi + \cos\Phi\sin\Theta\sin\Psi & \cos\Phi\cos\Theta \end{bmatrix}. \tag{30}$$

3.1. Vector form of equations of projectile motion in systems moving together with the projectile. Based on the law of change of momentum and angular momentum, spatial motion of the projectile as a rigid body can be described in the system moving together with the projectile and centered in the center of mass of the projectile with the following vector equations [2]:

$$m\left(\frac{\delta\mathbf{u}}{dt} + \boldsymbol{\Omega}_r \times \mathbf{u}\right) = \mathbf{R}^A + m\mathbf{g} + m\boldsymbol{\Lambda}, \tag{31a}$$

$$\frac{\delta\mathbf{H}}{dt} + \boldsymbol{\Omega}_r \times \mathbf{H} = \mathbf{M}_O^A, \tag{31b}$$

where $\boldsymbol{\Omega}_r$ – vector of angular velocity of the system moving together with the projectile relative to the normal earth axis system $Ox_g y_g z_g$, $\mathbf{R}^A = [X_a^A, Y_a^A, Z_a^A]$ – vector of aerodynamic force acting on the projectile and its components in the air-path axis system $Ox_a y_a z_a$, $\mathbf{M}_O^A = [L^A, M^A, N^A]$ – vector of aerodynamic moment acting on the projectile relative to its center of mass and its components in the body axis system $Oxyz$.

$$X_a^A = -i\left[C_{D_0} + C_{D_{\alpha^2}}(\sin^2\alpha + \sin^2\beta)\right]\frac{\rho v^2}{2}S, \tag{32a}$$

$$Y_a^A = \left[f_L(C_{L_\alpha} + C_{L_{\alpha^3}}\sin^2\beta)\sin\beta + C_{mag-f}\left(\frac{pd}{v}\right)\sin\alpha\right]\frac{\rho v^2}{2}S, \tag{32b}$$

$$Z_a^A = \left[-f_L(C_{L_\alpha} + C_{L_{\alpha^3}}\sin^2\alpha)\sin\alpha + C_{mag-f}\left(\frac{pd}{v}\right)\sin\beta\right]\frac{\rho v^2}{2}S, \tag{32c}$$

$$L^A = C_{spin}\left(\frac{pd}{v}\right)\ \frac{\rho v^2}{2}Sd, \tag{33a}$$

$$M^A = \left[(C_{M_\alpha} + C_{M_{\alpha^3}}\sin^2\alpha)\sin\alpha + C_{M_q}\left(\frac{qd}{v}\right) - C_{mag-m}\left(\frac{pd}{v}\right)\sin\beta\right]\frac{\rho v^2}{2}Sd, \tag{33b}$$

$$N^A = \left[(C_{M_\alpha} + C_{M_{\alpha^3}}\sin^2\beta)\sin\beta + C_{M_q}\left(\frac{rd}{v}\right) + C_{mag-m}\left(\frac{pd}{v}\right)\sin a\right]\frac{\rho v^2}{2}Sd. \tag{33c}$$

The scalar form of the foregoing vector equations (within appropriate coordinate systems), together with the complementary equations, represents a mathematical model of motion of the projectile as a rigid body in real conditions.

3.2. Mathematical model of the projectile motion in the body axis system *Oxyz*. If motion of the projectile is referred to the body axis system *Oxyz* overlapping with the principal central axes of inertia, the mathematical model of motion of the projectile as a rigid body can be described with the following groups of equations in the vector-matrix form:

– Dynamic differential equations of motion of the projectile center of mass

$$\begin{bmatrix}\dot u_x\\ \dot u_y\\ \dot u_z\end{bmatrix} = \mathbf{L}_{\alpha\beta}\begin{bmatrix}X_a^A/m\\ Y_a^A/m\\ Z_a^A/m\end{bmatrix} + \mathbf{L}_{\Phi\Theta\Psi}\begin{bmatrix}g_{x_g}+\Lambda_{x_g}\\ g_{y_g}+\Lambda_{y_g}\\ g_{z_g}+\Lambda_{z_g}\end{bmatrix} + \begin{bmatrix}0 & r & -q\\ -r & 0 & p\\ q & -p & 0\end{bmatrix}\begin{bmatrix}u_x\\ u_y\\ u_z\end{bmatrix}, \tag{34}$$

where

Components of Coriolis acceleration in the system $Ox_gy_gz_g$ have the following form:

$$\begin{bmatrix}\Lambda_{x_g}\\ \Lambda_{y_g}\\ \Lambda_{z_g}\end{bmatrix} = \begin{bmatrix}2\Omega\left(\cos(lat)\sin(AZ)u_{z_g} - \sin(lat)u_{y_g}\right)\\ 2\Omega\left(\cos(lat)\cos(AZ)u_{z_g} + \sin(lat)u_{x_g}\right)\\ -2\Omega\left(\cos(lat)\cos(AZ)u_{y_g} + \cos(lat)\sin(AZ)u_{x_g}\right)\end{bmatrix}. \tag{35}$$

For spherical model of the Earth, components of gravitational acceleration in the system $Ox_gy_gz_g$ can be expressed as follows [13]

$$\begin{bmatrix}g_{x_g}\\ g_{y_g}\\ g_{z_g}\end{bmatrix} = g_0\begin{bmatrix}-x_g/R_z\\ -y_g/R_z\\ 1+2z_g/R_z\end{bmatrix}. \tag{36}$$

– Kinematic differential equations of motion of the projectile center of mass

$$\begin{bmatrix}\dot x_g\\ \dot y_g\\ \dot z_g\end{bmatrix} = \begin{bmatrix}u_{x_g}\\ u_{y_g}\\ u_{z_g}\end{bmatrix} = \mathbf{L}^T_{\Phi\Theta\Psi}\begin{bmatrix}u_x\\ u_y\\ u_z\end{bmatrix}. \tag{37}$$

– Dynamic differential equations of rotational motion about the projectile center of mass in the body axis system *Oxyz* overlapping with the principle central axes of inertia

$$\begin{bmatrix}I_x & 0 & 0\\ 0 & I_y & 0\\ 0 & 0 & I_z\end{bmatrix}\begin{bmatrix}\dot p\\ \dot q\\ \dot r\end{bmatrix} = \begin{bmatrix}L^A\\ M^A\\ N^A\end{bmatrix} + \begin{bmatrix}0 & r & -q\\ -r & 0 & p\\ q & -p & 0\end{bmatrix}\begin{bmatrix}I_x & 0 & 0\\ 0 & I_y & 0\\ 0 & 0 & I_z\end{bmatrix}\begin{bmatrix}p\\ q\\ r\end{bmatrix}. \tag{38}$$

– Kinematic differential equations of rotational motion about the projectile center of mass

$$\begin{bmatrix}\dot\Psi\\ \dot\Theta\\ \dot\Phi\end{bmatrix} = \begin{bmatrix}0 & \sin\Phi/\cos\Theta & \cos\Phi/\cos\Theta\\ 0 & \cos\Phi & -\sin\Phi\\ 1 & \sin\Phi tg\Theta & \cos\Phi tg\Theta\end{bmatrix}\begin{bmatrix}p\\ q\\ r\end{bmatrix}. \tag{39}$$

– Equations for angle of attack α and angle of sideslip β

The equations can be derived by representing the components of vector $\mathbf{v}$ in the body axis system *Oxyz* with components in the air-path axis system $Ox_ay_az_a$

$$\begin{bmatrix}v_x\\ v_y\\ v_z\end{bmatrix} = \mathbf{L}_{\alpha\beta}\begin{bmatrix}v\\ 0\\ 0\end{bmatrix} \tag{40}$$

Using the transformation matrix (28), the components can be written in the following form

$$v_x = v\cos\alpha\cos\beta, \tag{41a}$$

$$v_y = -v\sin\beta, \tag{41b}$$

$$v_z = v\sin\alpha\cos\beta. \tag{41c}$$

Transforming Eq. (41b) provides an equation for the angle of sideslip:

$$\sin\beta = -\frac{v_y}{v}. \tag{42}$$

And dividing Eq. (41c) by Eq. (41a) provides an equation for the angle of attack

$$tg\alpha = \frac{v_z}{v_x}. \tag{43}$$

– Complementary equation

$$\gamma = \arcsin\frac{u_{z_g}}{u}, \qquad \chi = \operatorname{arctg}\frac{u_{y_g}}{u_{x_g}}, \tag{44}$$

$$\begin{gathered} v_x = u_x - w_x, \qquad v_y = u_y - w_y, \\ v_z = u_z - w_z, \end{gathered} \tag{45}$$

$$\begin{gathered} v = \sqrt{v_x^2 + v_y^2 + v_z^2}, \\ u = \sqrt{u_{x_g}^2 + u_{y_g}^2 + u_{z_g}^2}, \end{gathered} \tag{46}$$

where u , v – projectile velocity with respect to the ground and respect to the air, respectively, $[v_x, v_y, v_z]$ – components of vector of projectile velocity with respect to the air **v** in the body axis system *Oxyz*, $[u_x, u_y, u_z]$ – components of vector of projectile velocity with respect to the ground **u** in the body axis system *Oxyz*, $[u_{x_g}, u_{y_g}, u_{z_g}]$ – components of vector of projectile velocity with respect to the ground **u** in the normal earth axis system $Ox_gy_gz_g$, $[w_{x_g}, w_{y_g}, w_{z_g}]$ – components of vector of wind velocity with respect to the ground **w** in the normal earth axis system $Ox_gy_gz_g$, $[w_x, w_y, w_z]$ – components of vector of wind velocity with respect to the ground **w** in the body axis system *Oxyz*,

$$\begin{bmatrix} w_x \\ w_y \\ w_z \end{bmatrix} = \mathbf{L}_{\Phi\Theta\Psi} \begin{bmatrix} w_{x_g} \\ w_{y_g} \\ w_{z_g} \end{bmatrix}. \tag{47}$$

– Equations for initial conditions

$$u_x(t=0) = MV, \quad u_y(t=0) = 0, \quad u_z(t=0) = 0,$$
$$\Psi(t=0) = \Delta AZ, \quad \Theta(t=0) = QE, \quad \Phi(t=0) = 0.$$

3.3. Mathematical model of the projectile motion in the velocity axis system $Ox_ky_kz_k$. In this model, the dynamic differential equations of motion of the projectile center of mass have been derived in velocity axis system $Ox_ky_kz_k$ and the dynamic differential equations of rotational motion about the projectile center of mass in the body axis system *Oxyz*. The following is a complete system of equations:

– Dynamic differential equations of motion of the projectile center of mass in the velocity axis system $Ox_ky_kz_k$:

$$\begin{bmatrix} m\dot{u} \\ (mu\cos\gamma)\dot{\chi} \\ -mu\dot{\gamma} \end{bmatrix} = \mathbf{L}_{\gamma\chi}\mathbf{L}_{\Phi\Theta\Psi}^T\mathbf{L}_{\alpha\beta} \begin{bmatrix} X_a^A \\ Y_a^A \\ Z_a^A \end{bmatrix} + \mathbf{L}_{\gamma\chi} \begin{bmatrix} g_{x_g} + \Lambda_{x_g} \\ g_{y_g} + \Lambda_{y_g} \\ g_{z_g} + \Lambda_{z_g} \end{bmatrix}. \tag{48}$$

– Kinematic differential equations of motion of the projectile center of mass:

$$\begin{bmatrix} \dot{x}_g \\ \dot{y}_g \\ \dot{z}_g \end{bmatrix} = \begin{bmatrix} u_{x_g} \\ u_{y_g} \\ u_{z_g} \end{bmatrix} = \mathbf{L}_{\gamma\chi}^T \begin{bmatrix} u \\ 0 \\ 0 \end{bmatrix}. \tag{49}$$

– Dynamic and kinematic differential equations of rotational motion about the projectile center of mass (see Eqs. (38) and (39), respectively).

– Equations for components of vector of projectile velocity with respect to the air **v** in the body axis system *Oxyz*

$$\begin{bmatrix} v_x \\ v_y \\ v_z \end{bmatrix} = \mathbf{L}_{\Phi\Theta\Psi} \begin{bmatrix} u_{x_g} - w_{x_g} \\ u_{y_g} - w_{y_g} \\ u_{z_g} - w_{z_g} \end{bmatrix}. \tag{50}$$

– Equations for angle of attack α and angle of sideslip β (see Eqs. (43) and (42), respectively).

– Equations for initial conditions:

$$u(t=0) = MV, \quad \chi(t=0) = \Delta AZ, \quad \gamma(t=0) = QE,$$
$$\Psi(t=0) = \Delta AZ, \quad \Theta(t=0) = QE, \quad \Phi(t=0) = 0.$$

4. Results of numerical computations

Research into the effect of the mathematical model and integration step on the accuracy of the results of computation of artillery projectile flight parameters was done on an example of simulation of firing from a gun with the twist rate, $\eta = 20$ calibers, using Denel 155mm Assegai M2000 series artillery projectile (as the test projectile). See Fig. 3 for an overview and main dimensions, and Table 1 for physical characteristics, of the test projectile.

Table 2 specifies the aerodynamic characteristics of the test projectile computed using PRODAS 3.5.3 software application from Arrow Tech for:

$$p^* = pd/v, \quad q^* = qd/v, \quad r^* = rd/v$$
$$\text{and} \quad S = \pi d^2/4.$$

Linear interpolation was used for computing the values of aerodynamic characteristics between the nodal points.

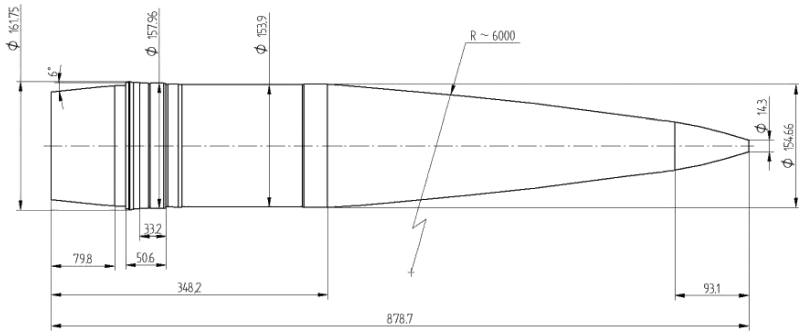

Fig. 3. Contour sketch of the Denel 155mm Assegai M2000 series projectile

Table 1
Physical characteristics of the Denel 155mm Assegai M2000 series projectile

Projectile diameter	d	0.155	m
Fuze projectile mass	m	43.7	kg
Center of gravity from nose	x_{CG}	0.563	m
Axial moment of inertia	I_x	0.1444	kgm^2
Transverse moment of inertia	I_y	1.7323	kgm^2

Table 2
Tabulated aerodynamic characteristics of the 155mm Assegai M2000 series projectile (STANAG 4355 ed3 aeroballistic nomenclature)

Ma	C_{D_0}	$C_{D_{\alpha^2}}$	C_{L_α}	$C_{L_{\alpha^3}}$	C_{mag-f}	C_{spin}	C_{M_α}	C_{mag-m}	C_{M_q}
[–]	[–]	[–]	[–]	[–]	[–]	[–]	[–]	[–]	[–]
0.010	0.144	3.520	1.480	−1.900	−0.425	−0.0154	3.755	−0.270	−4.75
0.400	0.144	3.520	1.480	−1.900	−0.425	−0.0154	3.784	−0.270	−4.60
0.600	0.144	3.540	1.490	−1.910	−0.425	−0.0154	3.774	−0.270	−4.75
0.700	0.144	3.730	1.490	−2.100	−0.430	−0.0154	3.763	−0.330	−4.90
0.800	0.146	3.960	1.510	−2.300	−0.440	−0.0154	3.785	−0.425	−5.50
0.900	0.160	4.480	1.590	−2.740	−0.475	−0.0153	3.843	−0.490	−7.00
0.950	0.202	4.990	1.700	−3.090	−0.600	−0.0148	3.825	−0.335	−8.40
0.975	0.240	5.260	1.720	−3.300	−0.535	−0.0146	3.736	−0.230	−9.40
1.000	0.284	5.510	1.720	−3.510	−0.495	−0.0145	3.577	−0.210	−10.40
1.025	0.313	5.780	1.760	−3.700	−0.475	−0.0145	3.570	−0.090	−10.90
1.050	0.332	6.000	1.800	−3.870	−0.460	−0.0146	3.558	0.055	−11.30
1.100	0.337	6.570	1.870	−4.360	−0.430	−0.0149	3.601	0.165	−11.40
1.200	0.340	7.150	1.960	−4.860	−0.390	−0.0151	3.675	0.260	−12.15
1.350	0.333	6.730	2.030	−4.370	−0.350	−0.0150	3.823	0.375	−12.80
1.500	0.321	6.320	2.100	−3.910	−0.340	−0.0146	4.014	0.410	−13.15
2.000	0.276	5.510	2.390	−2.850	−0.310	−0.0141	3.774	0.390	−14.05
2.500	0.240	5.030	2.550	−2.230	−0.305	−0.0134	3.583	0.340	−14.75
3.000	0.214	4.650	2.630	−1.810	−0.305	−0.0128	3.460	0.365	−14.70

Numerical computations made during the simulation of firing with the test projectile under different mathematical models used different integration steps. To solve the differential equations of motion the Runge-Kutta method has been used. The values of the particular trajectory parameters obtained for successive incremented integration steps have been used for computing errors produced by each integration step based on the following equations:

$$E_{r,h\mathbf{i}} = \frac{Par_{h\mathbf{i}} - Par_{h1}}{Par_{h1}} 100\%, \tag{1}$$

where $E_{r,h\mathbf{i}}$ – relative error in computation of particular trajectory parameters for i-th integration step relative to the parameters from step h_1, $Par_{h\mathbf{i}}$ – values of particular trajectory parameters obtained for step h_i.

The following were included as the particular trajectory parameters: X_{end} – range [m], y_{end} – drift [m], t_{end} – time of flight [s], V_{end} – final velocity of projectile [m/s], γ_{end} – angle of fall [mil], H_{max} – vertex [m].

Tables 3–5 show the results of computation of the particular trajectory parameters in standard conditions (International Standard Atmosphere [13]) obtained by simulating a flat trajectory ($QE = 200$ [mil]) and Tables 6–8 show the results for a steep trajectory ($QE = 1200$ [mil]), given the following initial conditions:

$$MV = 481 \text{ [m/s]}, \quad p_0 = 847.2 \text{ [rad/s]},$$
$$q_0 = 0 \text{ [rad/s]}, \quad r_0 = -1.9 \text{ [rad/s]}.$$

Table 3
Effect of integration step on accuracy of computation of the particular trajectory parameters of the projectile in the model based on the ground-fixed system for the flat trajectory (QE = 200 [mil])

	$h_1 = 0.00125$ [s]	$h_2 = 0.0025$ [s]	$\boldsymbol{h_3}$ **= 0.005** [s]	$h_4 = 0.01$ [s]	$E_{r,h2}$ [%]	$E_{r,h3}$ [%]	$E_{r,h4}$ [%]
X_{end} [m]	6164.5135	6164.5108	6164.4241	6161.9281	0.000	0.001	**0.042**
y_{end} [m]	34.0830	34.0830	34.0822	34.0576	0.000	0.002	**0.075**
t_{end} [s]	17.0414	17.0414	17.0413	17.0389	0.000	0.001	0.015
V_{end} [m/s]	309.8931	309.8930	309.8889	309.7715	0.000	0.001	**0.039**
γ_{end} [mil]	268.0926	268.0927	268.0950	268.1615	0.000	−0.001	**-0.026**
H_{max} [m]	362.6128	362.6127	362.6099	362.5311	0.000	0.001	**0.023**

Table 4
Effect of integration step on accuracy of computation of the particular trajectory parameters of the projectile in the model based on the velocity axis system for the flat trajectory (QE = 200 [mil])

	h_1 = 0.0001 [s]	$\boldsymbol{h_2}$ **= 0.0002** [s]	h_3 = 0.0004 [s]	h_4 = 0.0008 [s]	$E_{r,h2}$ [%]	$E_{r,h3}$ [%]	$E_{r,h4}$ [%]
X_{end} [m]	6164.4496	6164.5581	6164.7640	6163.0461	−0.002	−0.005	**0.023**
y_{end} [m]	34.0967	34.0998	34.1483	34.8188	−0.009	**−0.151**	**−2.118**
t_{end} [s]	17.0414	17.0414	17.0418	17.0376	0.000	−0.002	**0.022**
V_{end} [m/s]	309.8908	309.8909	309.8935	309.8857	0.000	−0.001	0.002
γ_{end} [mil]	268.0940	268.0942	268.0984	268.0740	0.000	−0.002	0.007
H_{max} [m]	362.6110	362.6119	362.6299	362.5560	0.000	−0.005	0.015

Table 5
Effect of integration step on accuracy of computation of the particular trajectory parameters of the projectile in the model based on the body axis system for the flat trajectory (QE = 200 [mil])

	h_1 = 0.000025 [s]	h_2 = 0.00005 [s]	$\boldsymbol{h_3}$ **= 0.0001** [s]	h_4 = 0.0002 [s]	$E_{r,h2}$ [%]	$E_{r,h3}$ [%]	$E_{r,h4}$ [%]
X_{end} [m]	6164.4503	6164.4706	6164.7960	6169.9909	0.000	−0.006	**−0.090**
y_{end} [m]	34.0965	34.0965	34.0999	34.2651	0.000	−0.010	**−0.494**
t_{end} [s]	17.0414	17.0414	17.0425	17.0600	0.000	−0.006	**−0.109**
V_{end} [m/s]	309.8908	309.8906	309.8874	309.8364	0.000	0.001	0.018
γ_{end} [mil]	268.0940	268.0943	268.0982	268.1630	0.000	−0.002	**−0.026**
H_{max} [m]	362.6111	362.6125	362.6360	363.0114	0.000	−0.007	**−0.110**

Table 6
Effect of integration step on accuracy of computation of the particular trajectory parameters of the projectile in the model based on the ground-fixed system for the steep trajectory (QE = 1200 [mil])

	h_1 = 0.00125 [s]	h_2 = 0.0025 [s]	$\boldsymbol{h_3}$ **= 0.005** [s]	h_4 = 0.01 [s]	$E_{r,h2}$ [%]	$E_{r,h3}$ [%]	$E_{r,h4}$ [%]
X_{end} [m]	9112.771	9112.7630	9112.4993	9105.0793	0.000	0.003	**0.084**
y_{end} [m]	573.0663	573.0655	573.0406	572.3381	0.000	0.004	**0.127**
t_{end} [s]	72.2363	72.2363	72.2356	72.2156	0.000	0.001	**0.029**
V_{end} [m/s]	318.5454	318.5451	318.5362	318.2845	0.000	0.003	**0.082**
γ_{end} [mil]	1294.1357	1294.1359	1294.1428	1294.3350	0.000	−0.001	−0.015
H_{max} [m]	6390.8858	6390.8819	6390.7549	6387.1735	0.000	0.002	**0.058**

Table 7
Effect of integration step on accuracy of computation of the particular trajectory parameters of the projectile in the model based on the velocity axis system for the steep trajectory (QE = 1200 [mil])

	h_1 = 0.0001 [s]	$\boldsymbol{h_2}$ **= 0.0002** [s]	h_3 = 0.0004 [s]	h_4 = 0.0008 [s]	$E_{r,h2}$ [%]	$E_{r,h3}$ [%]	$E_{r,h4}$ [%]
X_{end} [m]	9112.6954	9112.6975	9112.8361	9105.6282	0.000	−0.002	0.078
y_{end} [m]	575.3380	575.3759	575.9839	584.7120	−0.007	**−0.112**	**−1.629**
t_{end} [s]	72.2286	72.2286	72.2311	72.2295	0.000	−0.003	−0.001
V_{end} [m/s]	319.0354	319.0395	318.9534	316.1508	−0.001	**0.026**	**0.904**
γ_{end} [mil]	1294.2454	1294.2382	1294.1260	1293.1527	0.001	0.009	0.084
H_{max} [m]	6390.8126	6390.8275	6391.1622	6390.4171	0.000	−0.005	0.006

Table 8
Effect of integration step on accuracy of computation of the particular trajectory parameters of the projectile in the model based on the body axis system for the steep trajectory (QE = 1200 [mil])

	h_1 = 0.000025 [s]	h_2 = 0.00005 [s]	$\boldsymbol{h_3}$ **= 0.0001** [s]	h_4 = 0.0002 [s]	$E_{r,h2}$ [%]	$E_{r,h3}$ [%]	$E_{r,h4}$ [%]
X_{end} [m]	9112.6976	9112.7278	9113.1671	9118.8079	0.000	−0.005	**−0.067**
y_{end} [m]	575.3357	575.3453	575.6690	586.2775	−0.002	−0.058	**−1.902**
t_{end} [s]	72.2287	72.2295	72.2416	72.4336	−0.001	−0.018	**−0.284**
V_{end} [m/s]	319.0346	319.0351	319.0461	319.3948	0.000	−0.004	**−0.113**
γ_{end} [mil]	1294.2497	1294.2508	1294.3050	1295.1064	0.000	−0.004	**−0.066**
H_{max} [m]	6390.8137	6390.8416	6391.2889	6398.4636	0.000	−0.007	**−0.120**

5. Conclusions

The results of computations (see Tables 3–8 for example values) substantiate the following conclusions:

1) The same computation accuracy can be obtained for different models by using different maximum integration steps, provided that using quasi-Euler angles (Bryan angles) or quaternions in kinematic equations has no effect on the value of integration step;

2) To obtain a defined computation accuracy for the particular trajectory parameters of the projectile, the model based on the body axis system should use the smallest integration step, the model based on the velocity axis system should use a 5 times larger integration step and the model based on the ground-fixed system should use even 100 times larger integration step;

3) To obtain computation accuracy of 0.1% for drift (y_{end}) and 0.02% for the remaining parameters, the model based on the body axis system should use an integration step enabling approx. 100 computations per projectile revolution ($h = 0.01T$ where T – period of projectile rotation);

4) The computation results for the models based on the body axis and velocity axis systems are similar, but different from those provided by the model based on the ground-fixed system, specifically for the steep trajectory where total angle of attack α_t becomes larger than 10 [deg] on the trajectory vertex. The cause of the difference is that, for the model based on the ground-fixed system, aerodynamic forces and moments depend on total angle of attack α_t and the remaining models depend on angle of attack α and angle of sideslip β. Accordingly, total aerodynamic forces and moments computed using these models will be different because the following equation is true only for small angles of attack and sideslip:

$$\alpha_t \cong \sqrt{\alpha^2 + \beta^2};$$

5) The model based on the ground-fixed system, using direction cosines of the axes of symmetry of the projectile instead of quasi-Euler angles is the best mathematical model in terms of speed and computation accuracy. This model has one additional advantage: no singularities in the equations of motion, which happens in the other models for inclination angle of the projectile $\Theta = 90°$.

Acknowledgements. The research work was supported by the Polish Ministry of Science and Higher Education within years 2010–2013, under the grant 423/B0/A.

REFERENCES

[1] R.F. Lieske and R.L. McCoy, *Equations of Motion of a Rigid Projectile*, Ballistic Research Laboratories Report No. 1244, 1964.

[2] J. Gacek, *Exterior Ballistics. Part I. Modeling Exterior Ballistics and Flight Dynamics*, Military University of Technology, Warsaw, 1997, (in Polish).

[3] ISO 1151-1, *Flight Dynamics – Concepts, Quantities and Symbols – Part 1: Aircraft Motion Relative to the Air*, 1988.

[4] J. Gajda, "Using quaternions in algorithms for determining spatial orientation of moving objects", *Theoretical and Applied Mechanics* 28 (3–4), CD-ROM (1990), (in Polish).

[5] R.E. Roberson and R. Shwertassek, *Dynamics of Multibody System*, Springer-Verlag, Berlin, 1988.

[6] Z. Gosiewski and A. Ortyl, "Determining spatial orientation of aircraft using measurement of angular velocity vector", 6^{th} *Pol. Conf. on Mechanics in Aviation* 1, 191–215 (1995), (in Polish).

[7] R.L. McCoy, *Modern Exterior Ballistics. The Launch and Flight Dynamics of Symmetric Projectiles*, Schiffer Publishing, Atglen, 1999.

[8] G. Kowaleczko and A. Żyluk, "Influence of atmospheric turbulence on bomb release", *J. Theoretical and Applied Mechanics* 47 (1), 69–90, (2009).

[9] Z. Dziopa, I. Krzysztofik, and Z. Koruba, "An analysis of the dynamics of a launcher-missile on a moveable base", *Bull. Pol. Ac.: Tech.* 58 (4), 645–650 (2010).

[10] E. Ładyżyńska-Kozdraś and Z. Koruba, "Model of the final section of navigation of a self-guided missile steered by a gyroscope", *J. Theoretical and Applied Mechanics* 50 (2), 473–485 (2012).

[11] STANAG 4355 (Edition 3), *The Modified Point Mass and Five Degrees of Freedom Trajectory Models*, 2009.

[12] J. Shapiro, *Exterior ballistics*, Oborongiz, Moscow, 1946, (in Russian).

[13] ISO 2533, *The ISO Standard Atmosphere*, 1975.